Available online at www.sciencedirect.com
SCIENCE DIRECT®
Journal of Catalysis 225 (2004) 307–315
JOURNAL OF CATALYSIS
www.elsevier.com/locate/jcat

# Probing into the catalytic nature of Co/sulfated zirconia for selective reduction of NO with methane

Ning Li, Aiqin Wang, Mingyuan Zheng, Xiaodong Wang, Ruihua Cheng, and Tao Zhang *

*State Key Laboratory of Catalysis, Dalian Institute of Chemical Physics, Chinese Academy of Sciences, PO Box 110, Dalian 116023, China*

Received 12 February 2004; revised 12 April 2004; accepted 19 April 2004

**Abstract**

In this work, the structural and surface properties of Co-loaded sulfated zirconia (SZ) catalysts were studied by X-ray diffraction (XRD), $N_2$ adsorption, $NH_3$-TPD, FT-IR spectroscopy, $H_2$-TPR, UV–vis diffuse reflectance spectroscopy (DRS), X-ray photoelectron spectroscopy (XPS), and NO-TPD. $NH_3$-TPD and FT-IR spectra results of the catalysts showed that the sulfation process of the support resulted in the generation of strong Brønsted and Lewis acid sites, which is essential for the SCR of NO with methane. On the other hand, the $N_2$ adsorption, $H_2$-TPR, UV/vis DRS, and XPS of the catalysts demonstrated that the presence of the $SO_4^{2-}$ species promoted the dispersion of the Co species and prevented the formation of $Co_3O_4$. Such an increased dispersion of Co species suppressed the combustion reaction of $CH_4$ by $O_2$ and increased the selectivity toward NO reduction. The NO-TPD proved that the loading of Co increased the adsorption of NO over SZ catalysts, which is another reason for the promoting effect of Co.


*Keywords:* NO reduction; Methane; Co; Sulfated zirconia

## 1. Introduction

Oxides of nitrogen, as by-products of high-temperature combustion, cause serious environmental problems, such as acid rain and photochemical smog. Therefore, strict legislation around the world has led to the development of efficient $DeNO_x$ technologies in order to preserve the global environment. Over the last several years, the use of hydrocarbons as a substitute for ammonia in the selective catalytic reduction (SCR) of NO from oxygen-rich streams has drawn much attention [1–11]. Among various hydrocarbons, methane is the most preferable, because it is the main component of natural gas [5–11]. Many kinds of catalysts such as Co- [5,12–14], Ni- [13], Mn- [15–17], Ga- [18], In- [19–24], and Pd- [25,26] loaded ZSM-5 have been reported to be active for the catalytic reduction of NO with methane. However, water vapor and sulfur dioxide are typically present in combustion exhausts and may cause severe deactivation of catalysts for the SCR reaction [8,27–30]. Therefore, the development of new catalysts with higher tolerance toward the poisoning of water and $SO_2$ is very important.

Recently, we first investigated the catalytic performance of a series of nonnoble metal (Co, Mn, In, Ni)-loaded sulfated zirconia (SZ) for the SCR of NO with methane and found that Co exhibited the highest promoting effect on the activity of SZ catalysts among the investigated metals [31]. The optimum Co content of Co/SZ catalyst is about 4 wt%. Sulfation of support is necessary for the high activity and selectivity of Co/SZ catalysts. One of the most attractive features of Co/SZ catalysts is that they are less sensitive to water and $SO_2$ poisoning than Co/HZSM-5 catalysts and exhibited higher reversibility after removal of water or $SO_2$. In this work, to gain a deeper insight into the essence of the Co/SZ catalyst which is responsible for the good catalytic performance of the catalyst, and to understand the promoting effect of Co and $SO_4^{2-}$ for the SCR of NO with methane, we used a series of techniques to characterize the Co/SZ catalysts.

* Corresponding author. Fax: +86-411-84691570.
*E-mail address:* taozhang@dicp.ac.cn (T. Zhang).

0021-9517/$ – see front matter 
doi:10.1016/j.jcat.2004.04.026

## 2. Experimental

### 2.1. Catalyst preparation

Sulfated zirconia was prepared as described previously [31] by impregnating the precursor $Zr(OH)_4$ (AR grade, Shanghai Agent Company, China) with an aqueous solution of 0.5 M $(NH_4)_2SO_4$ in the ratio of 15 ml/g. The slurry was stirred slowly for half an hour, filtrated without washing, and dried at 110 °C overnight. Co/SZ was prepared by incipient wetness impregnation of the SZ with an aqueous solution of $Co(NO_3)_2$. For comparison, $Co/ZrO_2$ was prepared by the same method with $Zr(OH)_4$ as the support precursor. All the samples were dried at 110 °C for 8 h and calcined in air at 600 °C for 6 h. The $Co/ZrO_2$ catalyst as prepared was black in color, while the colors of Co/SZ catalysts varied with their Co contents: the colors of 2 wt% Co/SZ and 4 wt% Co/SZ were pink, the colors of 6 wt% Co/SZ and 8 wt% Co/SZ were, respectively, brown and black.

### 2.2. Characterization methods

#### 2.2.1. XRD measurements

XRD patterns were obtained with a Rigaku (D/MAX-$\beta$B) diffractometer equipped with an on-line computer. Ni-filtered Cu-K$\alpha$ radiation was used.

#### 2.2.2. BET surface area measurements

The specific surface areas of the catalysts were determined by nitrogen adsorption at 77 K using a Micromeritics ASAP 2010 apparatus. Before each experiment, the samples were evacuated at 150 °C for 3 h.

#### 2.2.3. $NH_3$-TPD measurements

$NH_3$-TPD of the catalysts was conducted with Micromeritics AutoChem II 2920 automated catalyst characterization system. A sample of 150 mg was placed in a quartz reactor and heated at 600 °C for 0.5 h in He flow to remove physically absorbed water. The adsorption of ammonia was performed at 100 °C. After saturation, the sample was heated linearly with a rate of 10 °C/min, from 100 to 650 °C under a constant He flow of 30 ml/min. The desorbed amount of ammonia was detected with a TCD detector.

#### 2.2.4. FT-IR spectroscopy measurements

The FT-IR spectra with pyridine as a molecular probe were recorded on a Nicolet Nexus 470 equipped with a liquid–nitrogen-cooled MCT detector at a resolution of 4 $cm^{-1}$ (64 scans). An adsorption IR cell allowed recording of the spectra at ambient temperature and catalyst activation at higher temperatures. The cell was equipped with a heater and connected to a vacuum system. The temperature was monitored with a thermocouple placed in direct contact with the sample. Self-supporting wafers (ca. 0.020 $g/cm^2$) of the samples were used for FT-IR studies. Before the surface characterization was performed, the samples were activated by heating in vacuum at 500 °C for 1 h, cooled down to ambient temperature, and saturated with pyridine vapor (at 0 °C) for 15 min. The spectra of the activated samples (taken at ambient temperature before adsorption of pyridine) were used as a background reference. Then, the samples were heated in vacuum at different temperatures for 1 h. The spectra of the samples that had been subjected to elevated temperatures were recorded after the IR cell had been cooled to ambient temperature. All of the spectra presented were obtained by subtraction of the corresponding background reference.

#### 2.2.5. $H_2$-TPR measurements

Temperature-programmed reduction (TPR) experiments were carried out with a Micromeritics AutoChem II 2920 automated catalyst characterization system using an $H_2$/Ar mixture (10% $H_2$). A catalyst charge of 150 mg was used. Before each experiment, the catalyst sample was pretreated at 600 °C in Ar flow for 0.5 h and then cooled to 40 °C. Subsequently, the Ar flow was switched to the $H_2$/Ar mixture, and the reduction was performed from 40 to 600 °C at a heating rate of 10 °C/min. The consumption of $H_2$ was determined with a TCD detector. Before the detector, a cold trap was used to remove the water generated in the reduction.

#### 2.2.6. UV–vis DRS measurements

DRS spectra were recorded in air in the wavelength range 200–800 nm on a JASCO V-550 spectrometer. The data were acquired and analyzed by a computer at the rate of 100 nm/min.

#### 2.2.7. XPS measurements

XPS spectra were recorded with a VG ESACALAB MK-2 X-ray photoelectron spectrometer, using Al-K$\alpha$ radiation (1486.6 eV, 12.5 kV, 250 W). Samples were ground in an agate mortar and pressed onto a gold-decorated tantalum plate attached to the sample holder. The analysis chamber was evacuated at pressures lower than $10^{-7}$ Pa. The computer collected sequentially the kinetic energy region of Co $2p_{1/2}$ and Co $2p_{3/2}$ (665–710 eV) and Zr $3d_{3/2}$ and Zr $3d_{5/2}$ (1290–1310 eV). Binding energy (BE) values were referenced to the Zr $3d_{5/2}$ peak taken as 182.5 eV.

#### 2.2.8. NO-TPD measurements

NO-TPD was conducted on a flowing reaction system using a mass spectrometer (Omini-star, GSD-300) as detector. Before the TPD experiment, the catalysts (300 mg) were pretreated at 600 °C in flowing He for 1 h, cooled to room temperature, and exposed to a gas stream of 1% NO in He at 50 ml/min to achieve saturated adsorption. Then, the catalysts were purged with He at 50 ml/min to remove gas-phase NO and weakly adsorbed NO. As the NO level, monitored by the mass spectrometer, returned to the background of the mass spectrometer, the TPD run was started from room temperature to 600 °C at a ramping rate of 15 °C/min. The

effluent gases from the reactor were continuously monitored as a function of temperature.

## 3. Results

### 3.1. XRD characterization

In this work, we investigated the effect of sulfation on the XRD patterns of catalyst. The XRD patterns of $ZrO_2$, 4 wt% Co/$ZrO_2$, SZ, and 4 wt% Co/SZ catalysts are shown in Fig. 1. All the samples that contain $SO_4^{2-}$, such as SZ and 4 wt% Co/SZ, have the same XRD patterns as that of tetragonal zirconia [32]. However, for the $ZrO_2$ and 4 wt% Co/$ZrO_2$ which have not been sulfated, the diffraction lines of monoclinic zirconia can also be observed [32]. These results demonstrate that the sulfation process is helpful for the stabilization of tetragonal zirconia. In addition, no distinct peaks of cobalt oxide can be observed after loading $ZrO_2$ or SZ with 4 wt% Co.

Furthermore, we compared the XRD patterns of Co/SZ catalysts with different Co contents. As shown in Fig. 2, the XRD patterns of the 2 wt% Co/SZ and 4 wt% Co/SZ catalysts are similar to that of SZ. While, in the XRD patterns of 6 wt% Co/SZ and 8 wt% Co/SZ, a weak peak of $Co_3O_4$ can be observed, respectively.

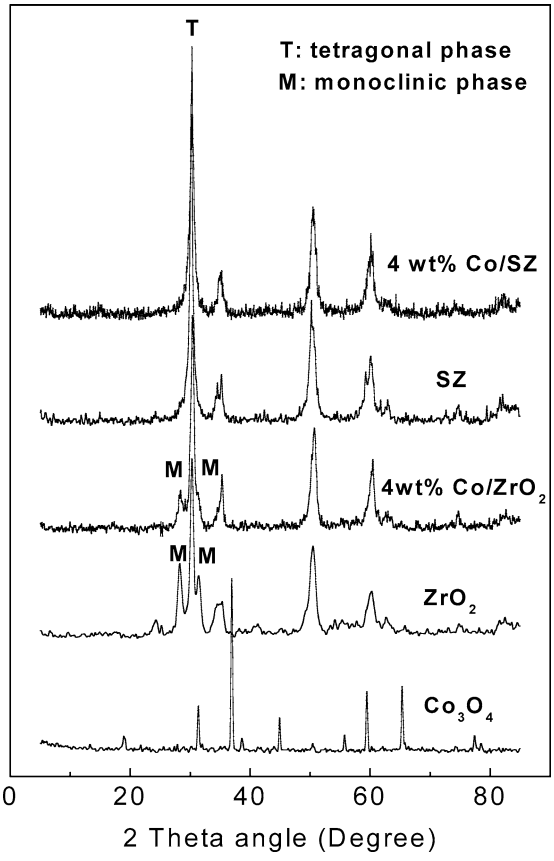


Fig. 1. XRD patterns of $ZrO_2$, SZ, 4 wt% Co/$ZrO_2$, 4 wt% Co/SZ, and $Co_3O_4$.

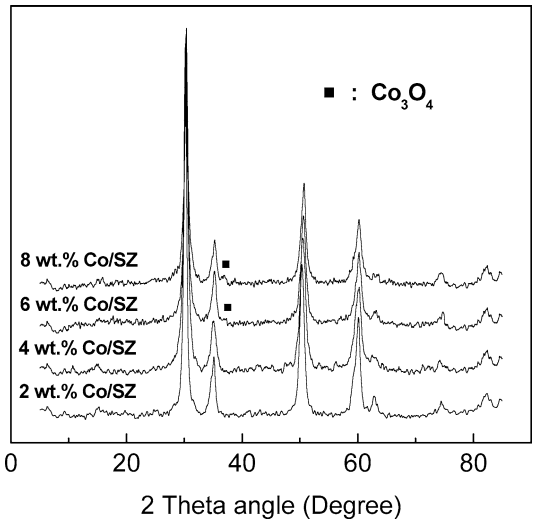


Fig. 2. XRD patterns of the Co/SZ catalysts with different Co contents.

Table 1
BET surface areas of the investigated catalysts

| Catalyst | BET surface area ($m^2/g$) |
|---|---|
| $ZrO_2$ | 45 |
| SZ | 94 |
| 4 wt% Co/$ZrO_2$ | 33 |
| 4 wt% Co/SZ | 83 |

### 3.2. BET characterization

Table 1 lists the BET surface areas of different catalysts. It is noticeable that sulfated samples such as SZ and Co/SZ have much greater surface areas than those of unsulfated ones ($ZrO_2$ and Co/$ZrO_2$), indicating that the sulfation process largely increased the surface areas of the catalysts. The difference in BET surface area between sulfated and unsulfated samples can be interpreted by the crystal phase. From the XRD result, it can be seen that the introducing of $SO_4^{2-}$ can restrain the phase transformation of the catalyst from a tetragonal phase to a denser monoclinic phase. This is the reason for the larger surface areas of sulfated samples. On the other hand, the loading of Co on the supports caused a slight decrease of the BET surface areas, as that of 4 wt% Co/$ZrO_2$ and 4 wt% Co/SZ compared with that of $ZrO_2$ and SZ, respectively.

### 3.3. $NH_3$-TPD and FT-IR spectroscopy characterization

It is generally accepted that the acid sites of catalysts play an important role in the SCR of NO with methane [33–39]. Therefore, in this work, we compared the $NH_3$-TPD spectra of different catalysts. From Fig. 3, it was evident that the amount of ammonia desorbed from pure zirconia was significantly increased by the sulfation. The spectrum of pure zirconia contained a very broad signal in the temperature range between 100 and 450 °C. Due to the sulfation, the intensity of the signal increased significantly and the tem-

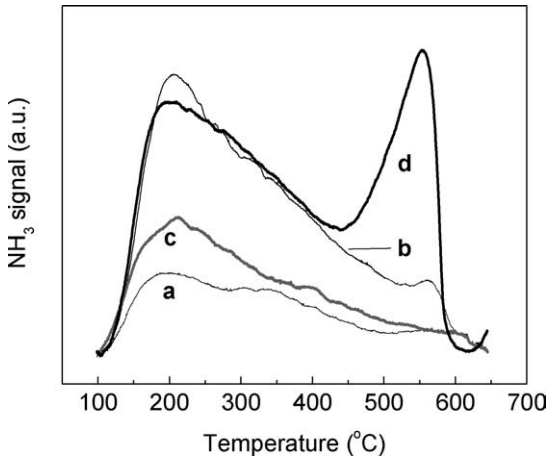


Fig. 3. $NH_3$-TPD spectra of (a) $ZrO_2$, (b) SZ, (c) 4 wt% $Co/ZrO_2$, and (d) 4 wt% Co/SZ.

perature window of ammonia desorption widened to 600 °C. Corma et al. [40] observed on sulfated zirconia an $NH_3$-TPD peak at 540 °C which they assigned to ammonia desorbed from strong acid sites. In this work, an evident peak can also be observed in the $NH_3$-TPD spectrum of our SZ at about 550 °C. Thereby, the conclusion can be drawn that sulfation of our zirconia led to the formation of strong acid sites as well. Moreover, it is very interesting that after loading SZ with Co a significant increase in the intensity of ammonia desorbed at higher temperature occurred, while the intensity of ammonia desorbed at lower temperature remained the same as its initial value. This result indicated that the introduction of Co increased the number of strong acid sites of SZ catalyst.

It is well known that the pyridine chemisorbed on Lewis and Brønsted acid sites will lead, respectively, to the adsorption bands at 1450 and 1540 $cm^{-1}$ in the infrared spectra [41,42], which is widely used to distinguish the type and relative quantity of the acid sites on the surface of catalysts. Therefore, in order to gain a deeper insight into the nature of the acid sites on different catalysts, we studied their FT-IR spectra with pyridine as a molecular probe. As shown in Fig. 4, the FT-IR spectra of both $ZrO_2$ and $Co/ZrO_2$ consisted only of bands of the Lewis acid–pyridine complex at about 1450 $cm^{-1}$. The intensities of such bands decreased with the evacuation temperatures and vanished after evacuation at 450 °C. It is clear that the $ZrO_2$ and $Co/ZrO_2$ possess predominantly weak Lewis acid sites. While, in the spectra of SZ and Co/SZ (cf. Fig. 5), evident bands of both Lewis and Brønsted acid can be observed; these bands still existed even after evacuation at 450 °C. These results indicate that the presence of $SO_4^{2-}$ leads to the generation of strong Lewis and Brønsted acid sites. On the other hand, it is noted that the Lewis–Brønsted ratio of the 4 wt% Co/SZ is higher than that of SZ. Such phenomenon is more pronounced after evacuation at 450 °C. Combining these results with those of $NH_3$-TPD, the conclusion can be drawn that the loading of Co increased the number of strong Lewis acid sites of

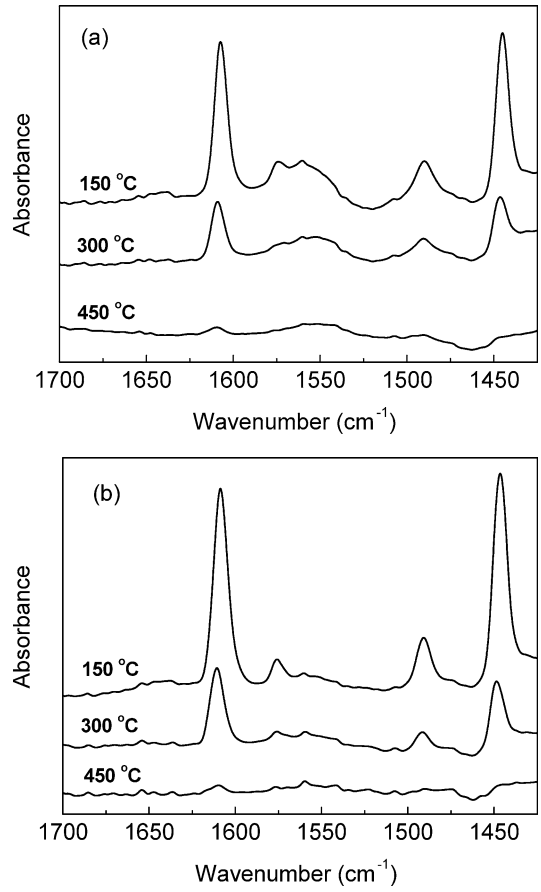


Fig. 4. The FT-IR spectra of pyridine adsorbed on $ZrO_2$ (a) and 4 wt% $Co/ZrO_2$ (b) after evacuation at different temperatures.

SZ catalysts. According to the literature [43,44], these new strong Lewis acid sites may be caused by the Co ions whose Lewis acid strength was increased owing to the electron-withdrawing effect of $SO_4^{2-}$.

Miller and co-workers [33,34] have investigated the role of acid sites in $Co^{2+}$-exchanged zeolite catalysts for selective catalytic reduction of $NO_x$. According to their opinion, the selective reduction of $NO_x$ with methane under lean conditions includes the following two steps:

$$2NO + O_2 \rightarrow 2NO_2, \quad (1)$$

$$2NO_2 + CH_4 \rightarrow CO_2 + 2H_2O + N_2. \quad (2)$$

NO oxidation is catalyzed predominantly by cobalt ions and cobalt oxides. By contrast, the formation of $N_2$ occurs at the strong Brønsted acid sites of catalysts by first protonation of the methane and then the reaction of adsorbed carbenium ions with gas-phase $NO_2$ leading to organo–nitrogen intermediates and the eventual formation of $N_2$. The rate of $N_2$ formation increases linearly with the number of strong Brønsted acid sites, and the specific rate increased with Brønsted acid strength. A similar conclusion was drawn by Kung and co-workers [35] based on the fact that the conversion of NO over a physical mixture of $Co/Al_2O_3$ and H-zeolite catalysts

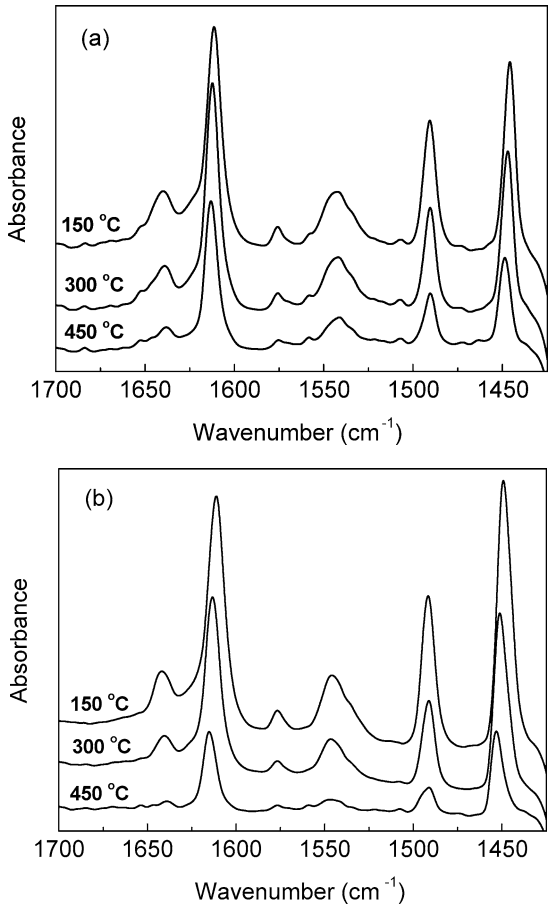


Fig. 5. The FT-IR spectra of pyridine adsorbed on SZ (a) and 4 wt% Co/SZ (b) after evacuation at different temperatures.

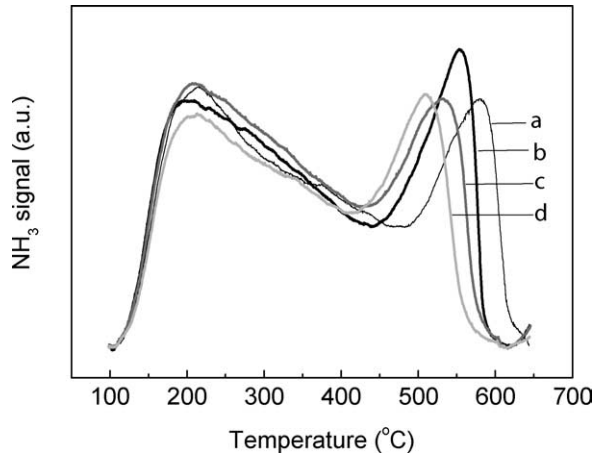


Fig. 6. $NH_3$-TPD spectra of (a) 2 wt% Co/SZ, (b) 4 wt% Co/SZ, (c) 6 wt% Co/SZ, and (d) 8 wt% Co/SZ.

was found to be twice that expected if these components acted independently.

In our case, it can be seen from the results of $NH_3$-TPD and FT-IR that the sulfation of zirconia will lead to the generation of strong Brønsted acid sites which can act as those of zeolites to protonate methane and facilitate the SCR of NO with methane by catalyzing the formation of $N_2$. Furthermore, we do not exclude the possibility that sulfation of support led to the generation of strong Lewis acid sites which may also play an important role in the SCR of NO with methane. Recently, Kantcheva et al. [45] studied the interaction between the $CH_4$ and the adsorbed $NO_x$ species over Co/SZ and Co/$ZrO_2$ with FT-IR spectra. According to them, methane can be adsorbed dissociatively over strong Lewis acid sites with the generation of strongly bound metal–alkyl or methoxy species [43,45]. Then, the formate species (formic acid) can be produced by fast oxidation of the methoxide. Such formate species plays a role of intermediates that are capable of selectively reducing NO.

Furthermore, we investigated the effect of Co content on the $NH_3$-TPD spectra of the Co/SZ catalysts as well. As shown in Fig. 6, the acidities of Co/SZ catalysts varied little when the Co content increased from 2 to 8 wt%. In our previous work [31], we have found that the activity of Co/SZ catalyst is strongly dependent on the Co loading. With the increase of Co content, the maximum NO conversion over Co/SZ increased initially, reached the highest value when the Co content is about 4 wt%, and then decreased. Moreover, the optimum temperature at which the maximum NO conversions were reached shifted to lower values. These results can be interpreted by Miller and co-workers [34] by the cooperation between Co and strong Brønsted acid sites of Co/SZ catalysts. When the Co content is low or at a low temperature, NO oxidation is slow and the rate-limiting step. Therefore, increasing the Co content will lead to the formation of more $NO_2$ and the increase of activity of Co/SZ catalysts. On the other hand, when the Co content is high or at a high temperature, the NO oxidation is in equilibrium, and excess Co will facilitate the nonselective reduction of $NO_2$ and decrease the selectivity of methane,

$$4NO_2 + CH_4 \rightarrow 4NO + CO_2 + 2H_2O,$$
$$2O_2 + CH_4 \rightarrow CO_2 + 2H_2O.$$

### 3.4. $H_2$-TPR characterization

$H_2$-TPR curves of different catalysts are presented in Fig. 7. Both pure $ZrO_2$ and SZ have no $H_2$ consumption peak at temperatures below 550 °C, indicating that the two supports were difficult to be reduced. After they were loaded with Co, different results were observed. For 4 wt% Co/$ZrO_2$ catalyst, a very wide $H_2$-TPR peak was observed in the temperature range between 300 and 450 °C. According to the literature [46–48], this wide peak can be attributed to the sequential reduction of $Co_3O_4$ to CoO and CoO to Co. In contrast, 4 wt% Co/SZ has only a peak at temperatures higher than 500 °C, which indicates that the presence of $SO_4^{2-}$ prevented the formation of $Co_3O_4$. This result can be explained by those of BET, $NH_3$-TPD, and FTIR because the sulfation process greatly increased the surface areas of the catalysts and generated strong Brønsted acid sites, such a dual effect of sulfation improved the dispersion of Co species and

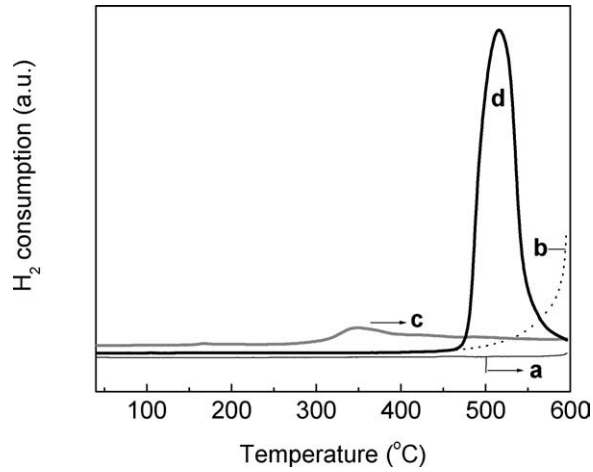


Fig. 7. $H_2$-TPR curves of (a) $ZrO_2$, (b) SZ, (c) 4 wt% Co/$ZrO_2$, and (d) 4 wt% Co/SZ.

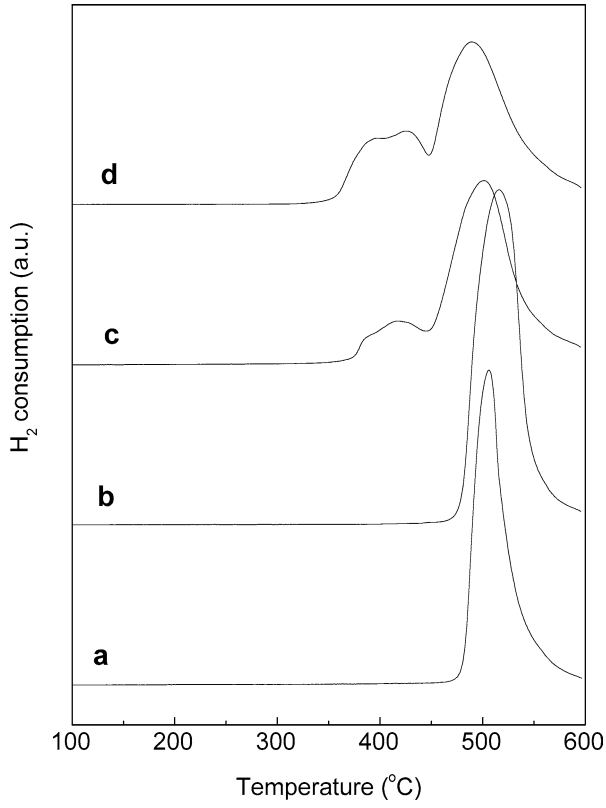


Fig. 8. $H_2$-TPR curves of (a) 2 wt% Co/SZ, (b) 4 wt% Co/SZ, (c) 6 wt% Co/SZ, and (d) 8 wt% Co/SZ.

prevented the formation of $Co_3O_4$ which is more easily reducible than dispersed Co species.

The next comparison that we have made is the $H_2$-TPR curves of Co/SZ catalysts with different Co contents. It can be seen from Fig. 8 that the maximum ability of SZ to disperse Co is about 4 wt%, when the Co content of Co/SZ catalyst is greater than this value, the peak of $Co_3O_4$ reduction will appear and its intensity increases with the Co

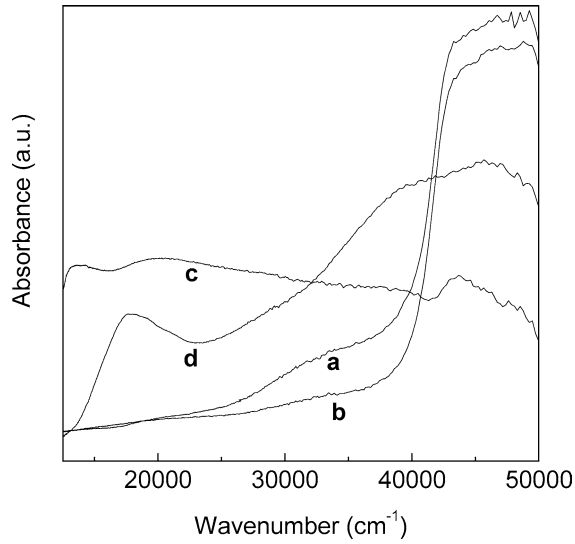


Fig. 9. UV/vis DRS spectra of (a) $ZrO_2$, (b) SZ, (c) 4 wt% Co/$ZrO_2$, and (d) 4 wt% Co/SZ.

content of the catalysts, which indicates the presence of increasing amounts of $Co_3O_4$.

### 3.5. UV–vis DRS characterization

Fig. 9 shows the DRS spectra of different catalysts. It can be seen that the spectra of $ZrO_2$ and SZ samples only consisted of a broad absorption at wavenumbers greater than 25,000 $cm^{-1}$. After loading them with 4 wt% Co, the results were completely different for $ZrO_2$ and SZ. Unlike pure $ZrO_2$, the spectrum of 4 wt% Co/$ZrO_2$ consisted of a weak band at about 14,000 $cm^{-1}$, indicating the presence of $Co_3O_4$ [44,49]. In contrast, the spectrum of 4 wt% Co/SZ consisted of a wide band in the wavenumber range between 16,000 and 21,000 $cm^{-1}$, absent on pure SZ. According to the literature [44,50], this peak can be attributed to typical $Co^{2+}$ in octahedral sites. These results can explain the great difference in the activities of Co/$ZrO_2$ and Co/SZ for the SCR of NO with methane from the nature of Co species. It is generally accepted that the $Co^{2+}$ is highly active for the SCR of NO with methane [51–56]. On one hand, $Co^{2+}$ can promote the oxidation of NO [33–35] and the formation of surface nitrates like that previously observed by Sachtler and co-workers on Co zeolites [54]. These nitrates are highly reactive toward methane [54,57]. On the other hand, as shown in the results of $NH_3$-TPD and IR, the presence of $Co^{2+}$ increases the number of strong Lewis acid sites of SZ catalysts. These strong Lewis acid sites may play a very important role for the partial oxidation of $CH_4$ and the SCR of NO [45]. $Co_3O_4$ is also very active for the oxidation of NO [33,56]. However, due to its high catalytic activity for the total oxidation of methane, it is unexpected for the SCR of NO [49,51,52].

Subsequently, we compared the DRS spectra of Co/SZ catalysts with different Co contents, and the results are shown in Fig. 10. It is clear that the DRS spectra of Co/SZ

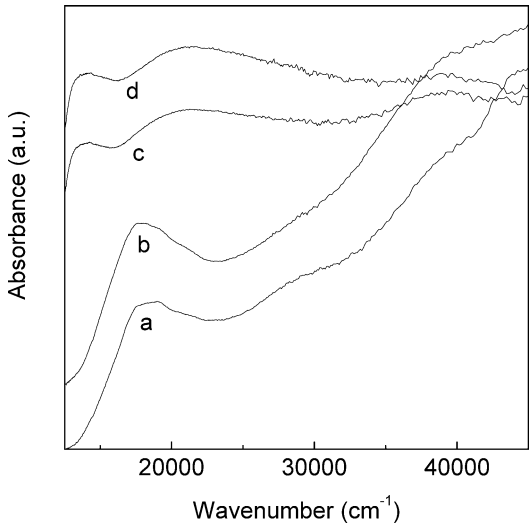


Fig. 10. UV/vis DRS spectra of (a) 2 wt% Co/SZ, (b) 4 wt% Co/SZ, (c) 6 wt% Co/SZ, and (d) 8 wt% Co/SZ.

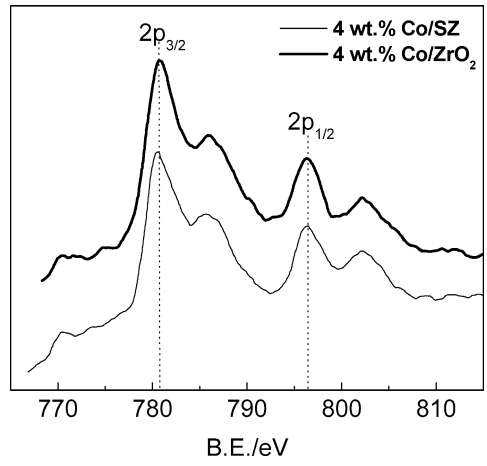


Fig. 11. XPS spectra of 4 wt% $Co/ZrO_2$ and 4 wt% Co/SZ catalysts.

Table 2
XPS parameters from Co 2p in $Co/ZrO_2$ and Co/SZ catalysts and relevant reference compounds

| Material | BE of Co $2p_{3/2}$ (eV) | $2p_{3/2} - 2p_{1/2}$ gap (eV) | Reference |
|---|---|---|---|
| CoO | 780.5 | 15.9 | [58] |
| $Co(OH)_2$ | 780.9 | 16 | [59] |
| $Co_3O_4$ | 780.7 | 15.0 | [58] |
| 4 wt% $Co/ZrO_2$ | 780.7 | 15.5 | |
| 4 wt% Co/SZ | 780.5 | 15.9 | |

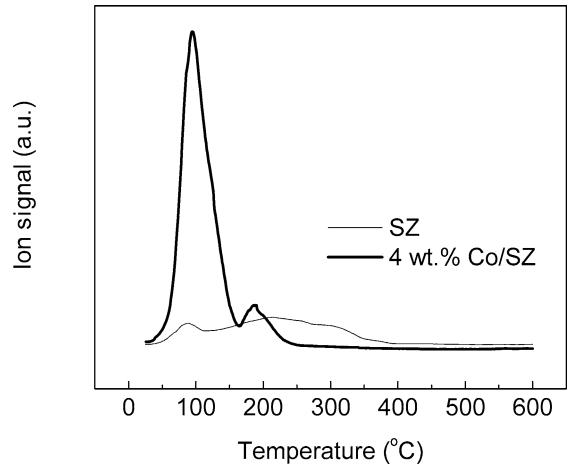


Fig. 12. NO-TPD profiles of SZ and 4 wt% Co/SZ catalysts.

catalysts with lower Co content ($\leqslant$ 4 wt%) only consisted of a wide band in the wavenumber range between 16,000 and 21,000 $cm^{-1}$, indicating that Co exists in the form of $Co^{2+}$ ions [44,50]. While, in spectra of the Co/SZ catalysts with Co content greater than 4 wt%, a band at about 14,000 $cm^{-1}$ appeared, indicating that these samples contained $Co_3O_4$. These results are consistent with those of $H_2$-TPR and can interpret the reason why the optimum Co content of Co/SZ is 4 wt% in another way: the maximum ability of SZ to anchor $Co^{2+}$ ions is about 4 wt%; when the Co content is beyond this value, Co will aggregate to $Co_3O_4$ and decrease the selectivity of $CH_4$ to NO reduction which will lead to the decrease of NO SCR activity of the catalyst.

### 3.6. XPS characterization

To further investigate the difference of Co species in $Co/ZrO_2$ and Co/SZ, we compared the XPS of 4 wt% $Co/ZrO_2$ and 4 wt% Co/SZ. As shown in Fig. 11 and Table 2, the XPS spectra of 4 wt% $Co/ZrO_2$ and 4 wt% Co/SZ samples are similar in shape and consist of two main bands at about 780 eV (Co $2p_{3/2}$) and 796 eV (Co $2p_{1/2}$), but there are still some differences in the BE for Co $2p_{3/2}$ and Co $2p_{3/2} - $ Co $2p_{1/2}$ gaps. For the Co/SZ sample, the BE value of Co $2p_{3/2}$ was found to be 780.5 eV, and the difference between the BE of Co $2p_{3/2}$ and Co $2p_{1/2}$ is 15.9 eV. These values are consistent with the literature values for CoO [58], indicating that the Co species in the 4 wt% Co/SZ mainly exists in a bivalent state. In contrast, for $Co/ZrO_2$, the BE value of Co $2p_{3/2}$ is 780.7 eV and the difference between the BE of Co $2p_{3/2}$ and Co $2p_{1/2}$ is 15.5 eV (between the value of CoO (15.9 eV) and that of $Co_3O_4$ (15.0 eV) [58]), indicating that a part of Co exists in the form of $Co_3O_4$. These results are in good agreement with those of $H_2$-TPR and DRS and give further proof that the presence of $SO_4^{2-}$ did prevent the formation of $Co_3O_4$ which is unexpected for the SCR of NO.

### 3.7. NO-TPD characterization

Fig. 12 shows the NO-TPD profiles of SZ and 4 wt% Co/SZ samples after the standard pretreatment. The NO-TPD profile of a SZ support has a wide peak range from room temperature to 350 °C. After loading it with 4 wt% Co, the intensity of the NO desorption peak of SZ was increased significantly, indicating that the introduction of Co increased the NO adsorption of SZ catalysts. This result can

elucidate the promoting effect of Co to the activity of SZ from an adsorption point of view.

In addition, it can be seen from Fig. 12 that the NO-TPD profile of a 4 wt% Co/SZ catalyst contains two peaks. According to the literature [60], the first peak at low temperature can be attributed to the NO desorption from $Zr^{4+}$–NO and $Co^{2+}(NO)_2$; the second peak at high temperature can be assigned to the NO desorption from the $Co^{n+}$–NO ($n = 2, 3$) species. Furthermore, it is found that the NO-TPD profile of our 4 wt% Co/SZ seems very similar to that obtained by Hadjiivanov et al. [60] on their highly dispersed Co/SZ sample (relative Co dispersion is 1.00), which reflects the high Co dispersion in our 4 wt% Co/SZ catalyst in another way.

## 4. Conclusions

It was demonstrated that both the sulfation of the supports and the metal loading played an important role in determining the catalytic performance of Co/sulfated zirconia catalysts. The sulfation process improved the dispersion of Co species and provided the strong Brønsted and Lewis acid sites which are essential for NO reduction. Both effects of sulfation maintained a high $CH_4$ selectivity toward NO reduction. Whereas, the loading of Co increased the number of strong Lewis acid sites and increased the NO adsorption of SZ, such dual effects of Co loading are responsible for its promoting effect for the SCR NO over SZ catalyst.

## Acknowledgments

Prof. Can Li, Pinliang Ying, Dr. Zhimin Liu, and Weicheng Wu are acknowledged for their great help in FT-IR spectroscopy characterization.

## References

[1] M. Iwamoto, in: Proceedings of Meeting of Catalytic Technology for Removal of Nitrogen Monoxide, Tokyo, Japan, 1990, p. 17.
[2] W. Held, A. Konig, T. Richter, L. Puppe, Soc. Automot. Eng. (1990), Paper 900 496.
[3] Y. Traa, B. Burger, J. Weitkamp, Micropor. Mesopor. Mater. 30 (1999) 3.
[4] V. Indovina, D. Pietrogiacomi, M.C. Campa, Appl. Catal. B 39 (2002) 115.
[5] Y. Li, J.N. Armor, Appl. Catal. B 1 (1992) L31.
[6] J.N. Armor, Catal. Today 26 (1995) 147.
[7] M.D. Fokema, J.Y. Ying, Catal. Rev.-Sci. Eng. 43 (2001) 1.
[8] Y.-H. Chin, A. Pisanu, L. Serventi, W.E. Alvarez, D.E. Resasco, Catal. Today 54 (1999) 419.
[9] Y.-H. Chin, W.E. Alvarez, D.E. Resasco, Catal. Today 62 (2000) 159.
[10] H. Ohtsuka, Appl. Catal. B 33 (2001) 325.
[11] J. Tang, T. Zhang, D. Liang, C. Xu, X. Sun, L. Lin, J. Chem. Soc., Chem. Commun. 19 (2000) 1861.
[12] X. Wang, H. Chen, W.M.H. Sachtler, Appl. Catal. B 29 (2001) 47.
[13] J. Tang, T. Zhang, L. Ma, L. Li, J. Zhao, M. Zheng, L. Lin, Catal. Lett. 73 (2001) 193.
[14] L. Ren, T. Zhang, D. Liang, C. Xu, J. Tang, L. Lin, Appl. Catal. B 35 (2002) 317.
[15] A.W. Aylor, L.J. Lobree, J.A. Reimer, A.T. Bell, J. Catal. 170 (1997) 390.
[16] M.C. Campa, D. Pietrogiacomi, S. Tuti, G. Ferraris, V. Indovina, Appl. Catal. B 18 (1998) 151.
[17] Q. Sun, W.M.H. Sachtler, Appl. Catal. B 42 (2003) 393.
[18] Y. Li, J.N. Armor, J. Catal. 145 (1994) 1.
[19] K. Yogo, E. Kikuchi, Stud. Surf. Sci. Catal. 84 (1994) 1547.
[20] X. Zhou, T. Zhang, Z. Xu, L. Lin, Catal. Lett. 40 (1996) 35.
[21] X. Zhou, Z. Xu, T. Zhang, L. Lin, J. Mol. Catal. A 122 (1997) 125.
[22] X. Wang, T. Zhang, X. Sun, W. Guan, D. Liang, L. Lin, Appl. Catal. B 24 (2000) 169.
[23] X. Wang, T. Zhang, C. Xu, X. Sun, D. Liang, L. Lin, J. Chem. Soc., Chem. Commun. 4 (2000) 279.
[24] L. Ren, T. Zhang, J. Tang, J. Zhao, N. Li, L. Lin, Appl. Catal. B 41 (2003) 129.
[25] C.J. Loughran, D.E. Resasco, Appl. Catal. B 7 (1995) 113.
[26] B. Wen, Q. Sun, W.M.H. Sachtler, J. Catal. 204 (2001) 314.
[27] Y. Li, P.J. Battavio, J.N. Armor, J. Catal. 142 (1993) 561.
[28] Y. Li, J.N. Armor, Appl. Catal. B 5 (1995) L257.
[29] P. Budi, E. Curry-Hyde, R.F. Howe, Stud. Surf. Sci. Catal. 105 (1997) 1549.
[30] Z. Li, M. Flytzani-Stephanopoulos, Appl. Catal. B 22 (1999) 35.
[31] N. Li, A. Wang, J. Tang, X. Wang, D. Liang, T. Zhang, Appl. Catal. B 43 (2003) 195.
[32] C. Morterra, G. Cerrato, F. Pinna, M. Signoretto, J. Catal. 157 (1995) 109.
[33] J.T. Miller, E. Glusker, R. Peddi, T. Zheng, J.R. Regalbuto, Catal. Lett. 51 (1998) 15.
[34] J.R. Regalbuto, T. Zheng, J.T. Miller, Catal. Today 54 (1999) 495.
[35] J.-Y. Yan, H.H. Kung, W.M.H. Sachtler, M.C. Kung, J. Catal. 175 (1998) 294.
[36] E. Kikuchi, K. Yogo, Catal. Today 22 (1994) 73.
[37] E. Kikuchi, M. Ogura, I. Terasaki, Y. Goto, J. Catal. 161 (1996) 465.
[38] M. Misono, Y. Nishizaka, M. Kawamoto, H. Kato, Stud. Surf. Sci. Catal. 105 (1997) 1501.
[39] H. Kato, C. Yokoyama, M. Misono, Catal. Today 45 (1998) 93.
[40] A. Corma, V. Fornes, M.I. Juan-Rajadell, J.M. Lopez Nieto, Appl. Catal. A 116 (1994) 151.
[41] B.H. Davis, R.A. Keogh, S. Alerasool, D.J. Zalewski, D.E. Day, P.K. Doolin, J. Catal. 183 (1999) 45.
[42] J.A. Lercher, C. Grundling, G. Eder-Mirth, Catal. Today 27 (1996) 353.
[43] M. Kantcheva, A.S. Vakkasoglu, J. Catal. 223 (2004) 352.
[44] D. Pietrogiacomi, M.C. Campa, S. Tuti, V. Indovina, Appl. Catal. B 41 (2003) 301.
[45] M. Kantcheva, A.S. Vakkasoglu, J. Catal. 223 (2004) 364.
[46] S.-J. Jong, S. Cheng, Appl. Catal. A 126 (1995) 51.
[47] X. Wang, H.-Y. Chen, W.M.H. Shachtler, Appl. Catal. B 26 (2000) L227.
[48] C. Resini, T. Montanari, L. Nappi, G. Bagnasco, M. Turco, G. Busca, F. Bregani, M. Notaro, G. Rocchini, J. Catal. 214 (2003) 179.
[49] D. Pietrogiacomi, S. Tuti, M.C. Campa, V. Indovina, Appl. Catal. B 28 (2000) 43.
[50] M. Che, F. Bozono-Verduraz, in: G. Ertl, H. Knozinger, J. Weitkamp (Eds.), in: Handbook of Heterogeneous Catalysis, vol. 2, Wiley, New York, 1997, p. 641.
[51] Y. Li, J.N. Armor, Stud. Surf. Sci. Catal. 81 (1994) 103.
[52] M.C. Campa, S.D. Rossi, G. Ferraris, V. Indovina, Appl. Catal. B 8 (1996) 315.
[53] M.C. Campa, I. Luisetto, D. Pietrogiacomi, V. Indovina, Appl. Catal. B 46 (2003) 511.
[54] B.J. Adelman, T. Beutel, G.-D. Lei, W.M.H. Sachtler, J. Catal. 158 (1996) 327.
[55] D. Kaucky, J. Dedecek, B. Wichterlova, Micropor. Mesopor. Mater. 31 (1999) 75.

[56] D. Kaucky, A. Vondrova, J. Dedecek, B. Wichterlova, J. Catal. 194 (2000) 318.
[57] B. Tsyntsarski, V. Avreyska, H. Kolev, T. Marinova, D. Klissurski, K. Hadjiivanov, J. Mol. Catal. A 193 (2003) 139.
[58] T.J. Chuang, C.R. Brundel, D.W. Rice, Surf. Sci. 59 (1976) 413.
[59] N.S. Mcintyoe, M.G. Cook, Anal. Chem. 47 (1975) 2208.
[60] K. Hadjiivanov, D. Panayotov, V. Avreyska, B. Tsyntsarski, D. Klissurski, T. Marinova, Surf. Interface Anal. 34 (2002) 88.